Hindawi
International Journal of Corrosion
Volume 2021, Article ID 6657160, 13 pages
https://doi.org/10.1155/2021/6657160

Research Article

Strength of Vegetated Coal-Bearing Soil under Dry-Wet Cycles: An Experimental Study

Gang Huang [1,2] **and Mingxin Zheng** [1]

[1] *Department of Civil Architecture College, East China Jiaotong University, Nanchang, China*
[2] *Department of Civil and Architecture Engineering, Huanggang Normal University, Huanggang, China*

Correspondence should be addressed to Mingxin Zheng; zhengmingxin0317@yeah.net

Received 25 December 2020; Revised 17 August 2021; Accepted 2 September 2021; Published 21 October 2021

Academic Editor: Ramana M. Pidaparti

Strength of vegetated coal-bearing soil is of great significance to evaluate the shallow stability of vegetated slopes in coal-bearing soil regions. This paper takes D-W cycles, dry density, water content, and vegetation root (VR) content as four factors and carries out the triaxial test for the orthogonal design of vegetated coal-bearing soil in southern China. The strength curves of vegetated coal-bearing soil under four factors were obtained. The Taguchi method was used to quantitatively analyse the effects of four factors. The microstructure of coal-bearing soil under D-W cycles and the theory of soil reinforcement by VR were discussed. The results indicated that D-W cycles had a significant effect on the cohesion and internal friction angle ($P < 0.05$). The internal friction angle was little affected by the water content and VR content, which had considerable influence on the cohesion. The cohesion could be improved with less than 2% VR content. The cohesion was the largest for no D-W cycles, 10% water content, and 2% VR content. The links between mineral particles go from a stable layered structure to unsteadiness chain structure with the increase in the number of D-W cycles.

1. Introduction

Coal-bearing soil, which consists of fully weathered carbonaceous mudstone or limestone weathered from coal-bearing strata, is poorly adhesive and easily expansive. With the rapid development of infrastructure in China, increasing quantities of coal-bearing soil are being weathered as coal-bearing strata are excavated during construction in southern China. Generally, coal-bearing soil is difficult to exploit because of its low raw coal content (low carbon content). Thus, the excavated coal-bearing soil layers typically remain in place and often experience shallow landslides during the rainy season, which can result in considerable harm to nearby traffic [1], which brings huge harm to traffic. The investigation found that the landslide was caused by atmospheric variation that caused fissures to accelerate the infiltration of rainwater [2]. Shallow landslides of coal-bearing soil were closely related to strength reduction [3]. Therefore, an urgent problem which could be solved is how to prevent fissures and improve the strength of coal-bearing soil [4]. So far, study on coal-bearing soil was fairly limited and mainly focused on the influence of water content on the strength characteristics of coal-bearing soil. The coal-bearing soil was sensitive to water [2, 5]. To address this issue, some researchers revealed that the cohesion of powered coal-bearing soil declines with water content increases in the form of exponential function [6]. The effect of water content on the shear strength of coal-bearing soil is related to the microstructure and conforms to the fractal theory [7]. Through scanning electron microscope scanning (SEM) and discrete element method (DEM), the microstructure characteristics of the coal-bearing soil with water content had an obvious variation [8, 9]. The repeated variety of water content could cause dry-wet (D-W) cycles, which was a well-known weathering process. Fissures gradually appear on the surface of the coal-bearing soil slope induced by D-W cycles. However, the study on D-W cycles of coal-bearing soil is still scarce.

In recent years, relative studies indicated that the protection of coal-bearing soil has gradually started to utilise vegetation ecological protection technology instead of traditional

engineering protection technology [10–12], mainly because of its significant role in reducing slope instability and erosion and improving the environment [13, 14]. The presence of vegetation could reduce the occurrence probability of shallow instability [15, 16]. Vegetation had been proven to be available for shallow slope stability, which is due to a series of hydrodynamic effects of vegetation roots (VR) and leaves [17]. A large number of studies have shown that the main effects of vegetation on slope stability were mechanical reinforcement and hydromechanical effects of VR [18]. Mechanical reinforcement refers to increasing the shear strength of the slope through the mechanical properties of VR, which improve the stability of slope soil and reduce the occurrence of the shallow landslide [19]. The role of VR in improving the shallow stability of the slope has been established through the tensile test, straight shear test, and triaxial test, etc. [20]. Hydrological effect refers to the absorption and transpiration of roots to increase the substrate suction of soil, thereby improving the stability of shallow slopes [21]. At present, research on the effects of hydrological on the stability of shallow slopes has become a hot topic. Relevant scholars in Hong Kong have conducted experiments to study the effect of roots on pore water pressure and the factor of safety (FOS) of a shallow slope in the atmospheric environment, moving towards the fundamental understanding of atmosphere-plant-soil interaction [22]. A mathematical model for the rate of root water uptake has been developed, including the root growth rate considering topographic factors, the type of vegetation, and climatic parameters [23, 24].

Existing studies have shown that the factors affecting soil strength mainly include water content, D-W cycles, and VR. In addition, dry density will affect the pore and permeability characteristics of the soil, and it will also affect soil strength indicators [25, 26]. However, the existing water content test studies only consider some of the above factors. Considering the dry density, D-W cycles, water content, and VR content, and introducing these influencing factors into the strong model of the coal-bearing soil, the triaxial test study has not been reported. Therefore, our study is the first attempt to understand the strength of the vegetated coal-bearing soil caused by the D-W cycles, dry density, water content, and VR content.

The aim of this paper is to understand the strength characteristics of the vegetated coal-bearing soil. This article takes vegetated coal-bearing soil as a research object and conducts a large number of D-W cycle triaxial compression tests. The effects of dry density, D-W cycles, water content, and VR content on the strength of compacted coal-bearing soil are comprehensively considered in the test. The microstructures were analysed by SEM test, and the digital model of soil reinforcement by VR was established. The research conclusions can provide a reference for the analysis of strength characteristics of vegetated coal- bearing soil and slope shallow protection.

2. Materials and Methods

2.1. Sample Preparation. The research object is the vegetated coal-bearing soil in Shangli County district of the Changli Expressway (Figure 1). The Changli Expressway is the most convenient passageway between the capital cities of Hunan and Jiangxi provinces. The project was located in the western Jiangxi region and belongs to the humid subtropical monsoon climate. Summer accounts for 40% of annual precipitation, and it is the rainy season from mid-May to mid-July. The annual average precipitation was about 1603, and the maximum monthly precipitation was about 165. The rainfall was large and concentrated, which adversely affected the stability of the slope.

The coal-bearing soil specimens were taken out with a shovel and placed in a plastic bag to seal storage. The indoor soil property test determined that the dry density of the reshaped coal-bearing soil was 1.55 g/cm^3, the optimal water content was 10.5% (geotechnical test method standard GBT 50123-2019), the liquid limit was 10.5%, the liquid limit was 14.1%, and the plasticity index was 9.1%; the grain size composition is shown in Table 1. The unevenness coefficient Cu was 27.5, and the curvature coefficient Cc was 2.64. The engineering classification of coal-bearing soil was SW according to the Unified Soil Classification System, ASTM D 2487-10 [27], which was a well-graded soil.

The coal-bearing soil specimens were first placed in an oven at 105°C for 24 hours to ensure that coal-bearing soil specimens could be dried. The dried coal-bearing soil was crushed and passed through a two-millimeter sieve. The sieved coal-bearing soil was sprayed with water in layers with the optimal water content of 10% and left to stand for 2 hours to make the water uniform in coal-bearing soil specimens. Finally, the coal-bearing soil and simulated VR (hemp rope) were made into a standard triaxial sample with a diameter of 39.1 mm and a height of 80 mm by a geotechnical test method, as shown in Figure 2.

2.2. D-W Cycle Process. Triaxial tests were performed after the coal-measure-soil specimens were subjected to 1, 2, 3, 4, and 5 dry-wet cycles. The D-W cycles includes two steps: drying and wetting. The process of drying and wetting under atmospheric conditions due to rainwater infiltration, water table rise, and transpiration is similar to 1D water migration. Furthermore, the water-content gradient influences the development characteristics of soil fissures. To simulate the influence of D-W cycles on the shear strength of soil under natural conditions, we adopted the method of approximately simulating 1D moisture transfer. During drying and wetting, the sides of the specimen were wrapped with a rubber film, which ensured that water in the soil could be transferred through the upper and lower sides of the specimen. The D-W cycling process used in the study was as follows: heating for 8 h at 70°C→water injection for 4 h→heating for 8 h at 70°C→water injection for 4 h. The total period of each cycle was 12 h. The water content of the specimens during D-W cycles was controlled at a time by controlling the total amount of the specimen, and the accuracy was ±0.1 g.

2.3. Simulation of VR. The effect of VR in the shallow layer of the slope could play the role of mechanical reinforcement on the soil. The VR had great differences in morphology and properties according to different vegetated species. The

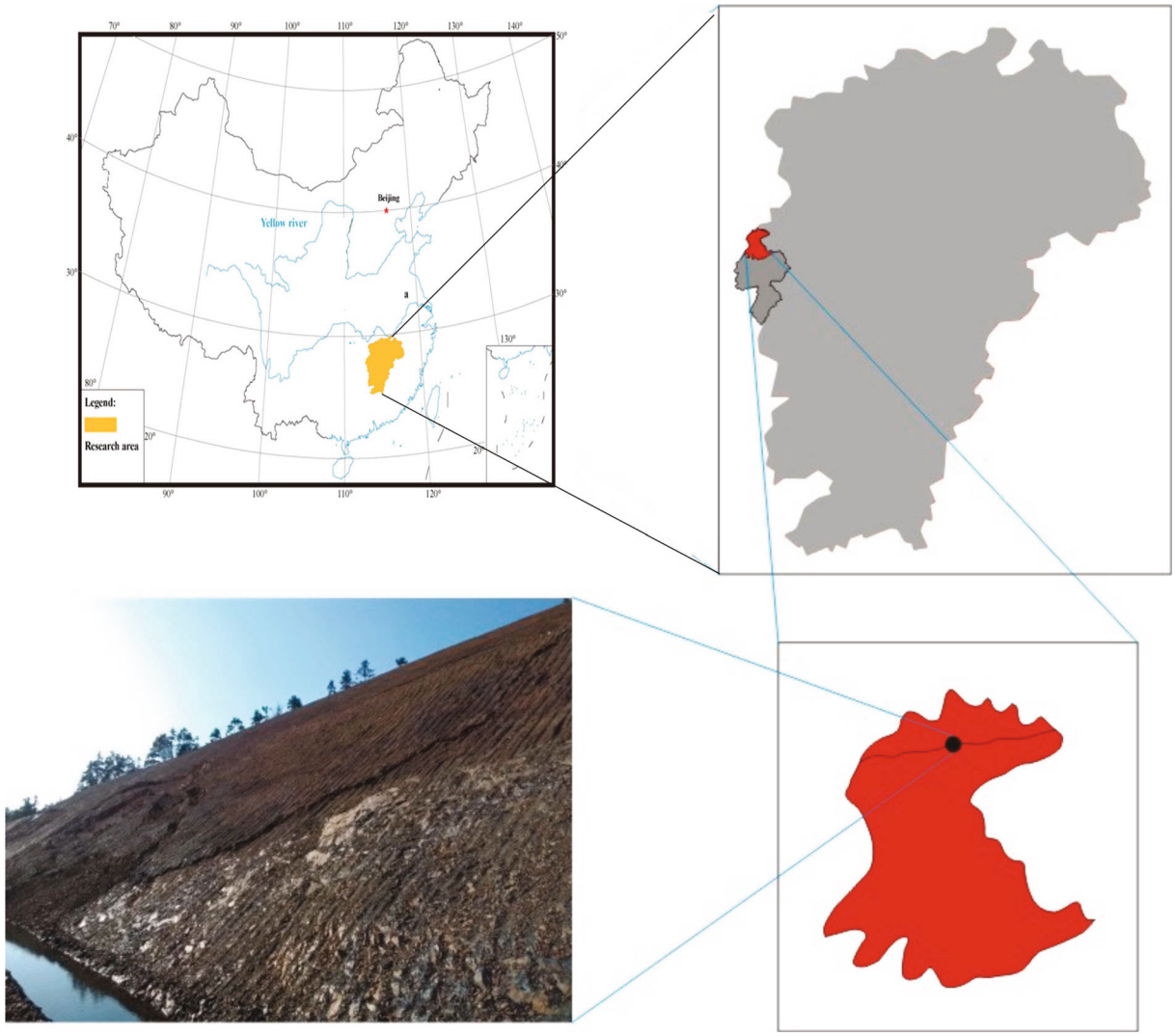

Figure 1: Sampling location.

Table 1: Grain size composition of powdered coal-bearing soil.

Grain size range (mm)	Content (%)	Grain size range (mm)	Content (%)
>5	7.8	0.5~0.25	9.6
5~2	4.1	0.25~0.075	8.5
2~0.5	54.6	<0.075	15.4

tensile strength of VR was between 5 MPa and 100 MPa (tensile test), the plastic deformation was 2%-3%, and the deformation modulus is 100-6000 kPa [28, 29]. The hemp rope was made of vegetated material. Because hemp rope is made from plant material, its mechanical properties are basically the same as those of plant roots, and it can mimic the roots of different plant species. Root bending resistance was not considered according to the direction of prevention. Through the tensile test, the average tensile strength was 35 MPa, and the plastic deformation was 2%. The hemp rope was selected as the root simulation material, which was consistent with the general VR characteristics. The hemp rope was arranged one quarter away from the two ends of the sample in three layers. Each layer was arranged in three sections, which was the chiasma type, as shown in Figure 3.

2.4. Orthogonal Experimental Design and Taguchi Method. For undisturbed vegetated soil, the difference in dry density affects the strength index of powdery coal-bearing soil [30]. Therefore, it is of practical significance to study the effect of dry density on the strength effect of vegetated coal-bearing soil.

The influence degree and regularity of the number of D-W cycles N, dry density ρ, water content w, and VR content R on the strength of vegetated coal-bearing soil were analysed. Variables and values are shown in Table 2. The water content w and VR content R were percent by weight. In this paper, the triaxial test of the vegetated coal-bearing soil adopted the orthogonal test method. By using the method of extremum and variance, the influence degree and significance level of each factor on the strength parameters were ranked. Orthogonal design is shown in Table 3.

Figure 2: The specimen of triaxial text.

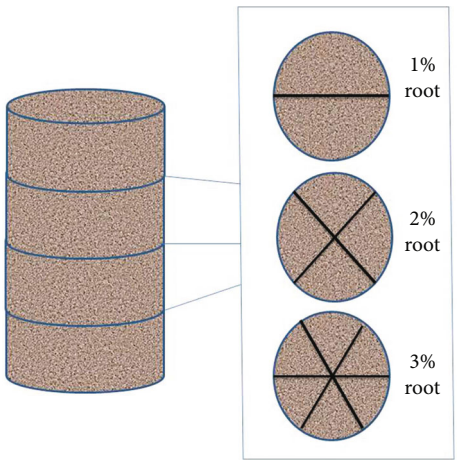

Figure 3: The arrangement of the rope in the sample.

Table 2: Variables and values.

Level	Variables			
	N	w (%)	R (%)	ρ (g/cm^3)
1	0	5	0	1.45
2	1	10	1	1.50
3	3	15	2	1.55
4	5	20	3	1.60

The effects of the four considered factors (N, ρ, w, and R) on the strength index were calculated using an analysis of variance (ANOVA) with Duncan's multiple range test and paired t-tests. Correlations with P values less than 0.05 were considered significant. All statistical tests were performed using SPSS Statistics 23.

The Taguchi method utilises an orthogonal array to design experiments and analyse the data. The method has been widely used in scientific experiments, quality control, and manufacture [31, 32]. It was specially developed to check the relative importance of multivariables, as listed in Table 4.

Table 3: Orthogonal design.

Test #	N	w (%)	R (%)	ρ (g/cm^3)
1	0	5	0	1.45
2	0	10	1	1.50
3	0	15	2	1.55
4	0	20	3	1.60
5	1	5	2	1.50
6	1	10	3	1.45
7	1	15	0	1.60
8	1	20	1	1.55
9	3	5	3	1.55
10	3	10	2	1.60
11	3	15	1	1.45
12	3	20	0	1.50
13	5	5	1	1.60
14	5	10	0	1.55
15	5	15	3	1.50
16	5	20	2	1.45

The equipment for the test was the Tsz-3 triaxial strain control system (Figure 4). The loading mode was that of displacement loading; the loading rate was 0.01 mm/s.

3. Triaxial Test Results

3.1. Stress-Strain Curves. The stress-strain $(\sigma_1\text{-}\sigma_3)\varepsilon_1$ curves of each group were obtained through triaxial tests of unconsolidated and nondrained (UU) powdered coal-bearing soil under the action of D-W cycles. The stress-strain curves of different numbers of D-W cycles are plotted in Figure 5. The peak shear stress or the shear stress of 15% axial strain (there is no peak) of the stress-strain curves was taken as the shear strength.

It can be seen from the stress-strain curves in Figure 5 that the shear stress increases with increasing strain. The stress-strain curves show a nonlinear relationship. With increasing stress, the strain softening increments rapidly increase. The more the numbers of D-W cycles, the smaller the shear strength. This is because D-W cycles change the arrangement of particles in the sample soil, and the bite force of particles decreases.

3.2. Shear Strength Parameters

3.2.1. Cohesion. To investigate the effect of four factors on cohesion, the relationship between the factor and cohesion is plotted in Figure 6.

As plotted in Figure 6(a), when the number of D-W cycles was less than one, the relationships between the number of D-W cycles and cohesion were not obvious. When the water content was greater than one, the cohesion was decreasing with the increase in the number of D-W cycles. D-W cycles had a great influence on the cohesion of coal-

Table 4: Examples of Taguchi's method for range analysis.

Test	Variable A	Variable B	Variable C	Evaluated parameter
1	A1	B1	C1	Y1
2	A1	B2	C2	Y2
3	A2	B1	C2	Y3
4	A2	B2	C1	Y4
K1	Y1+Y2	Y1+Y3	Y1+Y4	
K2	Y3+Y4	Y2+Y4	Y2+Y3	
Vi	2	2	2	
$\overline{K_1}$	K1/Vi	K1/Vi	K1/Vi	
$\overline{K_2}$	K2/Vi	K2/Vi	K2/Vi	
Range (R)	$\mathrm{Max}\{\overline{K_1}, \overline{K_2}\}$- $\mathrm{min}\{\overline{K_1}, \overline{K_2}\}$			

Figure 4: Triaxial test.

bearing soil ($P < 0.05$).The cohesion decreases up to 13.2 kPa for every D-W cycle. It indicated that D-W cycles were very sensitive to the strength of vegetated coal-bearing soil. This is because coal-bearing soil shrunk and expanded repeatedly. When the environment is drying, the water molecules in clay minerals in vegetated coal-bearing soils begin to evaporate, and the soils shrink and structural damage occurs beyond a certain threshold. When the environment turns wet, the structural damage of vegetated coal-bearing soil is accelerated by the wedge pressure of water and the expansion pressure of clay minerals [33].

As plotted in Figure 6(b), when the water content is less than 10%, the cohesive force increases as the water content increases. However, when the water content was greater than 10%, with the increase of water content, the cohesion was decreasing. When the water content was 10%, the cohesion was the maximum. The water has an influence on the cohesion of vegetated coal-bearing soil ($P < 0.05$). When the water content was large, the cohesion decreases up to 3 kPa for every 1% increase in water content. It indicated that water was also affecting the strength of vegetated coal-bearing soil. Water and coal-bearing soil interactions were intense, leading to a decrease in strength and landslide [2].

As plotted in Figure 6(c), when the VR content was less than 2%, the cohesion slowly increases. When the VR content was greater than the critical value, the cohesive force decreased as the VR content increased.

As plotted in Figure 6(d), the relationship between dry density and cohesion was not very significant ($P > 0.05$). According to the average cohesion, it was found that with the increase of dry density, the cohesion change amplitude was only 10 kPa, which shows that the effect of dry density was not significant ($P > 0.05$).

To investigate the effect of four influencing factors on cohesion, the analysis of cohesion was carried out, as listed in Table 5. Range of D-W cycle was 53.6. The D-W cycles were the dominating factor affecting cohesion, followed by VR content and water content. Dry density had little effect on the cohesion. From the above data, the range of D-W cycles was twice as large as the other factors. When the number of D-W cycles was over one, the swelling force of coal-bearing soil is under dry conditions, and liquid bridge force is under wet conditions, the liquid bridge force has reached a threshold repeatedly, resulting in the occurrence of the fissure, which is reducing the cohesion. When the roots were in the proper amount, the VR exerts its tensile properties, which was beneficial to the cohesion of coal-bearing soil. When a lot of VR impede the adhesion of coal-bearing soil, it was easy to form a weak surface at the simulated interface. Therefore, VR reduces coal-bearing soil cohesion. When the water content was 10%, the VR content effect was obvious, which results in the stable internal structure of coal-bearing soil. Besides, when the water content was over 10%, the contact surfaces between the water and the soil were increased, resulting in the available decrease in cohesion. As for the small effect of dry density and cohesion, the possible reason was that the increase in dry density only reduced the voids of coal-bearing soil and did not increase the cohesiveness of soil particles. The amount of dry density did not cause the deterioration of coal-bearing soil to be significant, and it is difficult to affect the cohesion.

3.2.2. Internal Friction Angle. To investigate the effect of four factors on the internal friction angle, analysis of the internal friction angle was carried out, as listed in Table 6. It can be seen that the order of Table 6 is slightly different from that of Table 5. The D-W cycles were still the main factors affecting the internal friction angle, and the effect of VR content was undermined. The relationship between the number of D-W cycles and the internal friction angle is plotted in Figure 7. According to Figure 7, the internal friction angle decreased with the increasing number of D-W cycles ($P < 0.05$). However, the internal friction angle slowly increased with the increasing number of D-W cycles after reaching a valley value of 19.9°. It indicated that the variation

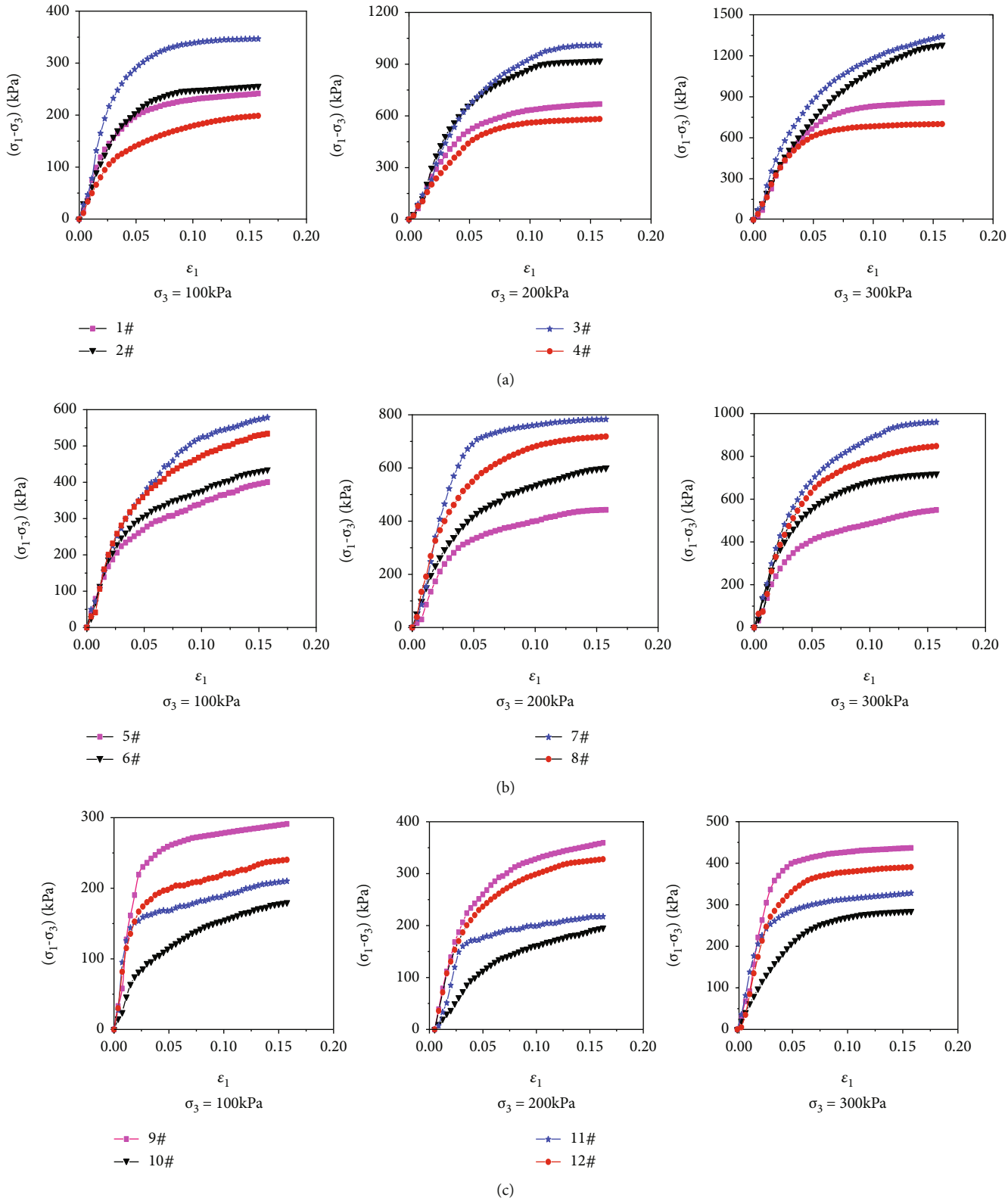

Figure 5: Continued.

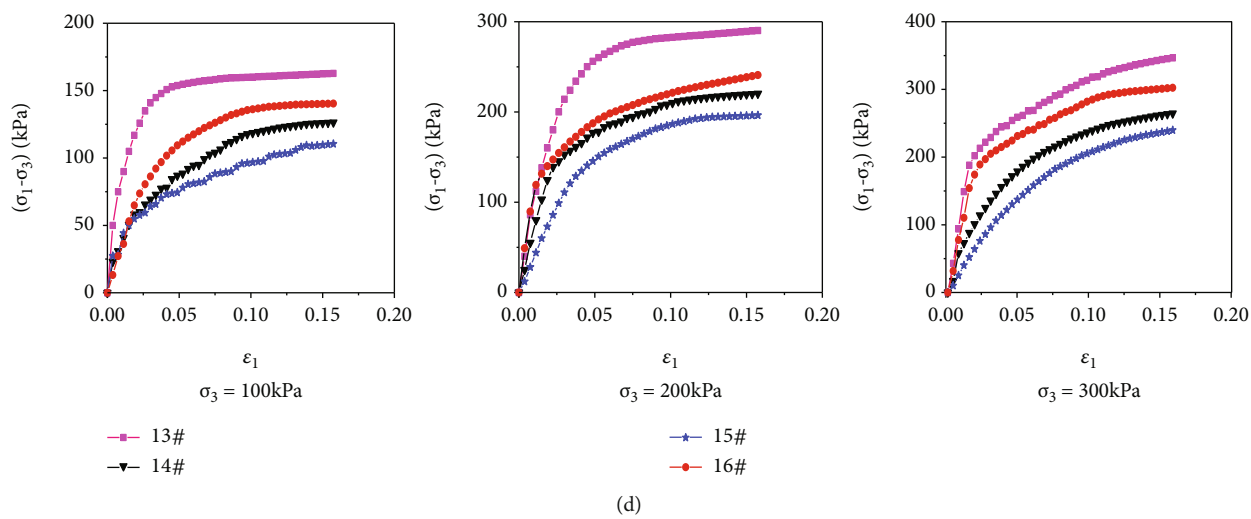

Figure 5: The stress-strain curves variation of vegetated coal-bearing soil specimens: (a) no D-W cycles; (b) one D-W cycles; (c) three D-W cycles; (d) five D-W cycles.

of the atmospheric environment for coal-bearing soil particles causes the particles to wear and fissure, reducing the internal friction angle. The range of cohesion for D-W cycles was more than twice the internal friction angle. The effect of the water content on cohesion degeneration was not as significant as that of D-W cycles.

4. Discussion

4.1. Microstructure Characterization Affected by D-W Cycles. Research on geotechnical microstructure using SEM has become the most common geotechnical technique [34]. Many studies show that the strength properties of soil are closely related to the microstructure [35, 36]. To study the relationship between water and coal-bearing soil, the mineral composition and chemical composition are analysed by Sigma 300 scanning electron microscopy (SEM). Figure 8 is a comparison of the microstructure of powdered coal-bearing soil before and after the D-W cycles. As the D-W cycles increase, small pores increase and microfractures can also be clearly observed. Notably, several edge-to-edge contacts can be observed between mineral particles. Chain structures at the edges of clay minerals can be observed. It is inferred that the D-W cycles have caused the basic structural units and contact relationships of the particles to readjust; the links between mineral particles have stable layered structures through surface-to-surface contact to chain structures through edge-to-edge, which is different from Han et al. [8] in microstructure change. The microstructure from surface-to-surface to surface-to-edge contact was studied under different levels of water content. It can be seen from the figure that the D-W cycles have caused the basic structural units and contact relationships of the particles to change. Clay minerals had the high swelling-shrinking ability under D-W cycle conditions [37–39].

As the number of D-W cycles increases, the number of edge debris increased. The degree of particle fragmentation and the pores increase visibly. With increase of the number of D-W cycles, the contact relationship gradually changed from surface-to-surface contact to edge to-edge contact. The multiplication of pores and the development of microcracks simultaneously affected the shear strength. The microcracks provided the necessary conditions for water and coal-bearing soil interaction [40]. The variation of the basic structural unit and contact relationship of the particles caused the strength softening of the powdery coal-bearing soil. The water was a polar molecule and a solvent. Coal-bearing soil contains a variety of soluble components, such as clay minerals. Clay minerals had high expansive characteristics under D-W cycle conditions (Figure 9). When the environment was drying, the water molecules in clay minerals in coal-bearing soils began to evaporate and the soil shrink, and structural damage occurred beyond a certain threshold. When the environment turned wet, the structural damage of coal-bearing soil was accelerated by the wedge pressure of water and the expansion pressure of clay minerals, and microcracks appear. Some particles began to separate from the coal with the washing effect of water. After dry-wet cycles, the clay mineral particles were clustered together under the interaction of liquid bridge force and interparticle force [41].

4.2. Theoretical Analysis of Soil Reinforcement by Vegetation Roots

4.2.1. Theoretical Analysis. Vegetation can protect the slope from shallow landslides, mainly because the underground root system strengthens the surface soil. When the coal-bearing soil slope has frequent rainfall in the south of the Yangtze River in summer, on the one hand, the erosion chain formed under the erosive force of the rainfall will bring the soil particles down the slope; on the other hand, the permeable layer will be formed after the water infiltrates, reducing the soil resistance. The shear strength affects the stability of the shallow soil of the slope. This section combines the basic theory of unsaturated soils, establishes a

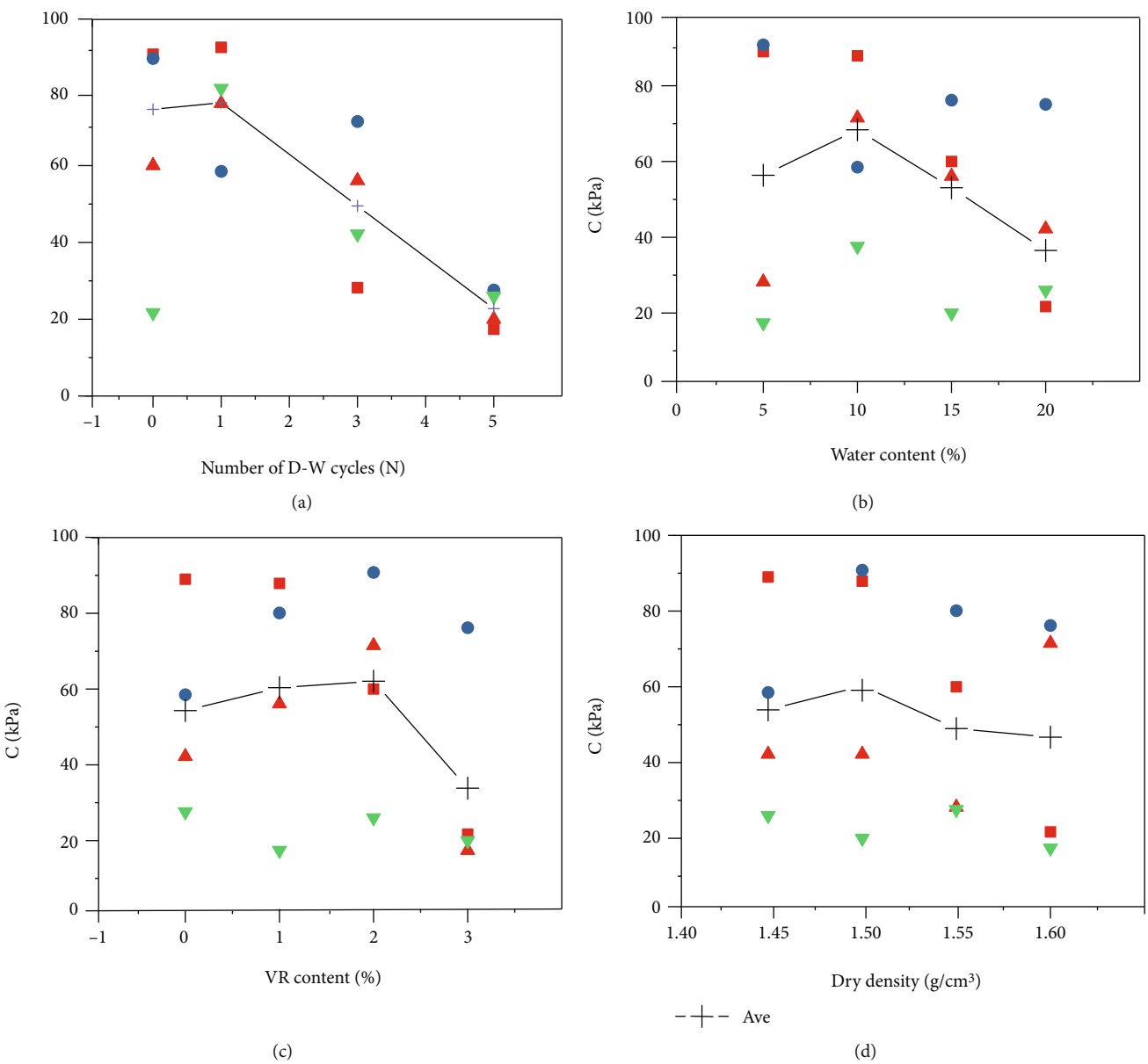

FIGURE 6: (a) Cohesion vs. number of W-D cycles; (b) cohesion vs. water content; (c) cohesion vs. VR content; (d) cohesion vs. dry density.

mathematical formula to explain the root failure mechanism and analyses the reinforcement mechanism of roots on unsaturated soils.

The formula for the shear strength τ_f of unsaturated soil is

$$\tau_f = c' + (\sigma - u_a)\tan\phi' + (u_a - u_w)\left[\tan\phi'\left(\frac{\theta - \theta_r}{\theta_s - \theta_r}\right)\right], \quad (1)$$

where c' and ϕ' are the effective cohesion and the effective angle of internal friction of soil mass, respectively; $\sigma - u_a$ is the net stress of unsaturated soil; $u_a - u_w$ is the matric suction; θ, θ_r, and θ_s are the current, residual, and saturated moisture contents of the soil, respectively.

The cohesion c' of the root-soil is mainly composed of two parts: (1) the effective cohesion c_s' of the soil; (2) the cohesion $\Delta c_r'$ induced by the root system, namely,

$$c' = c_s' + \Delta c_r'. \quad (2)$$

According to the improvement of the Wu model by Preti and Schwarz [42], the root-induced cohesion $\Delta c_r'$ is

$$\Delta c_r' = 0.4 \cdot \mathrm{RAR} \cdot T_N \delta, \quad (3)$$

where RAR is the root area ratio, T_N is the maximum tensile

Table 5: Range analysis for cohesion.

Test #	N	w (%)	R (%)	ρ (g/cm^3)	c (kPa)
1	0	5	0	1.45	89
2	0	10	1	1.50	87.9
3	0	15	2	1.55	60
4	0	20	3	1.60	21.7
5	1	5	2	1.50	90.8
6	1	10	3	1.45	58.5
7	1	15	0	1.60	76.2
8	1	20	1	1.55	80.1
9	2	5	3	1.55	28.2
10	2	10	2	1.60	71.5
11	2	15	1	1.45	56.1
12	2	20	0	1.50	42.2
13	3	5	1	1.60	17.4
14	3	10	0	1.55	27.6
15	3	15	3	1.50	20
16	3	20	2	1.45	26
$\overline{K_1}$	64.7	56.4	54.3	53.9	
$\overline{K_2}$	76.4	61.4	60.4	60.2	
$\overline{K_3}$	49.5	53.1	62.1	49.0	
$\overline{K_4}$	22.8	42.5	33.8	46.7	
Range	53.7	18.9	28.3	13.5	

Table 6: Range analysis for internal friction angle.

Test #	N	w (%)	R (%)	ρ (g/cm^3)
$\overline{K_1}$	39.7	26.7	26.3	26.6
$\overline{K_2}$	32.2	27.2	30.2	25.2
$\overline{K_3}$	19.9	30.6	30.0	35.1
$\overline{K_4}$	23.4	30.7	30.0	29.4
Range	19.8	4.0	3.9	9.9

stress caused by the root, and δ is a parameter related to the root direction, which can be expressed as

$$\delta = \cos\alpha_i + \sin\alpha_i \tan\phi', \tag{4}$$

where α_i is the angle of the first deforming root to the horizontal plane.

The model is extended to estimate the contribution of plant roots to the cohesive force increase $\Delta c_r'$ under a certain displacement, by considering the root failure mode observed in the triaxial test which is the cohesive force $\Delta c_r'$ produced by elongated roots.

According to Figure 10(a), the vertical slip length ΔL of the root is

$$\Delta L = L_2 - \left(L - L_1 - \sqrt{\left(\Delta d^2 + \Delta t^2\right)}\right), \tag{5}$$

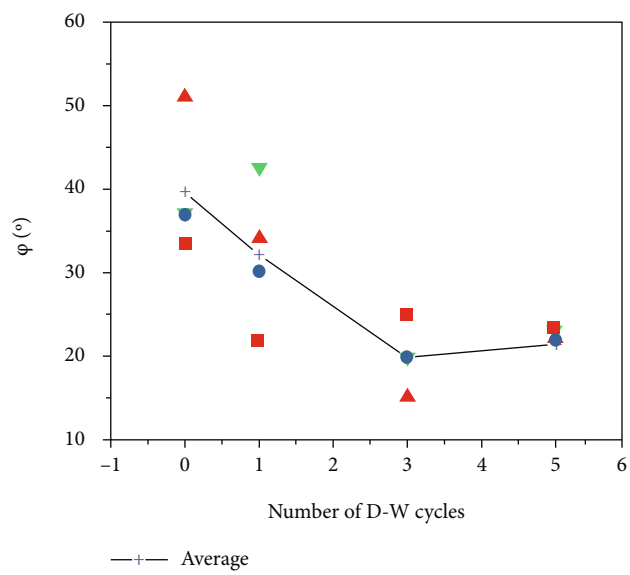

Figure 7: The relationship between the number of D-W cycles and internal friction angle.

where L_1 is the root which has no vertical length of horizontal movement and L_2 is the vertical length of the horizontal movement of the root.

It can be seen from Figure 10(b) that the inclination angle α_2 between the deformed root and the horizontal is

$$\tan\alpha_2 = \frac{\Delta t}{\Delta t/\tan\beta + \Delta d}, \tag{6}$$

where Δd is the shear displacement, Δt is the shear length of the root, and β is the angle of the shear segment of the root deformation.

The elongation of the roots ω is

$$\omega = \frac{L_2 - \left(L - L_1 - \sqrt{\left(\Delta d^2 + \Delta t^2\right)}\right)}{L}. \tag{7}$$

The energy generated by the root elongation is

$$E = \frac{1}{2} T_i \omega = \frac{1}{2} k e^2, \tag{8}$$

where k is the elastic modulus of the root and e is the root elongation.

Tensile stress generated by the i tensile root is

$$T_i = k\left[\frac{L_2}{\sin\alpha_2} + \left(L - \frac{L_1}{\sin\alpha_2} - \sqrt{(\Delta t\tan\alpha_2 + \Delta d)^2 + \Delta t^2}\right)\right]. \tag{9}$$

The cohesion Δc_r produced by root elongation is

$$\Delta c_r = 0.4 \cdot \sum_{i=0}^{m_1} \mathrm{RAR}_i \cdot T_i \cdot \left(\cos\alpha_i + \sin\alpha_i \tan\phi'\right), \tag{10}$$

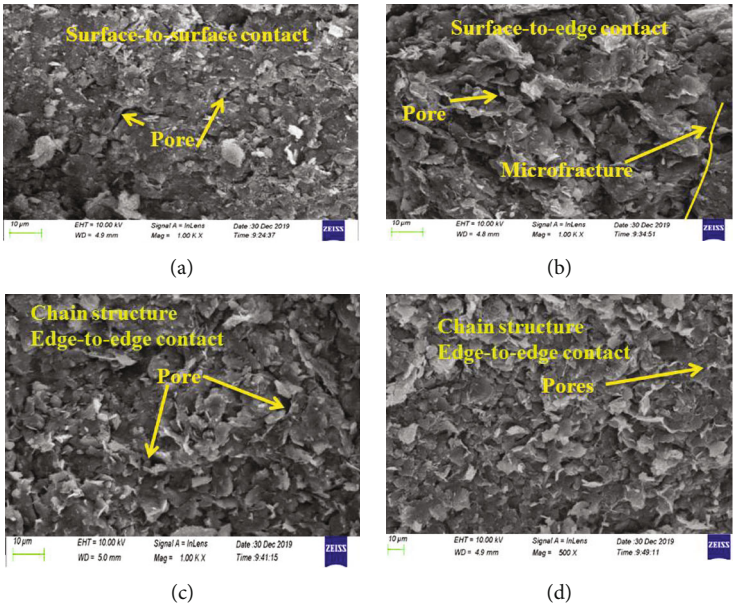

Figure 8: SEM image at a magnification of 1000: (a) no D-W cycles; (b) one D-W cycles; (c) three D-W cycles; (d) five D-W cycles.

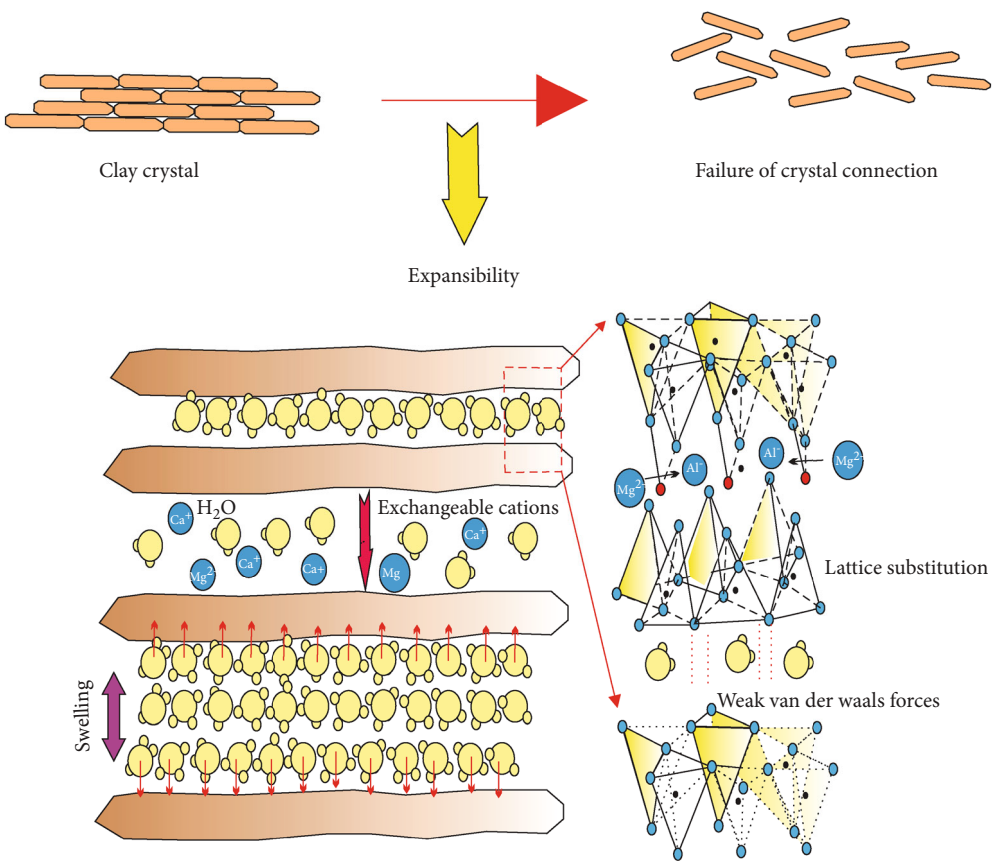

Figure 9: Coal-bearing soil with expansive characteristics.

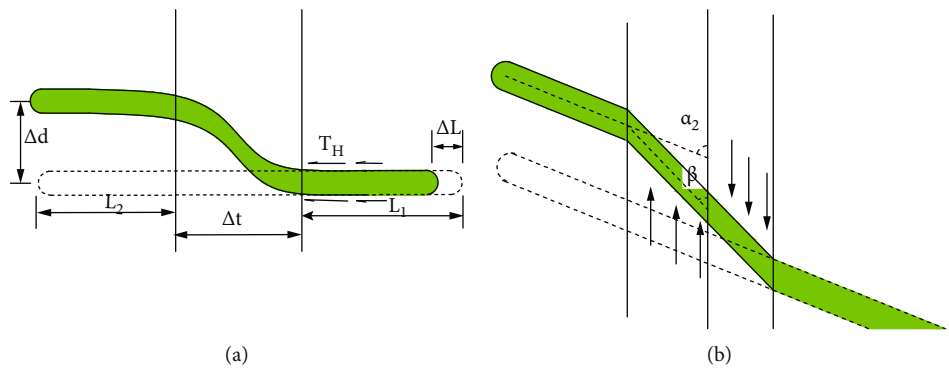

Figure 10: Schematic diagram of root stress and deformation: (a) vertical root deformation; (b) inclined root deformation.

Table 7: Root parameters.

Diameter (cm)	Elasticity modulus (kN/m^2·mm^{-1})	Length (cm)	Shear thickness (cm)	L_1 (cm)	L_2 (cm)	Δd (cm)	Mobile length (cm)	Tensile strength (kN/m^2)	Mean soil depth (cm)
0.3	10000	17	2	7.6	7.6	1.4	0.93	10000	2.9
0.21	10000	14	2	6.3	6.3	1.4	0.93	10000	2.6
0.12	10000	10	2	4.6	4.6	1.4	0.23	10000	2.0
0.34	10000	9	2	2.5	2.5	1.4	0.23	10000	4.4
0.23	10000	15	2	8.6	8.6	1.4	0.93	10000	2.1
0.62	10000	15	2	12.3	12.4	1.4	0.93	10000	42.6
0.52	10000	15	2	9.6	9.6	1.4	0.23	10000	2.0
0.3	10000	15	2	2.5	2.5	1.4	0.23	10000	2.4
0.21	10000	15	2	9.6	9.6	1.4	0.23	10000	2.0
0.34	10000	15	2	2.5	2.5	1.4	0.23	10000	2.4

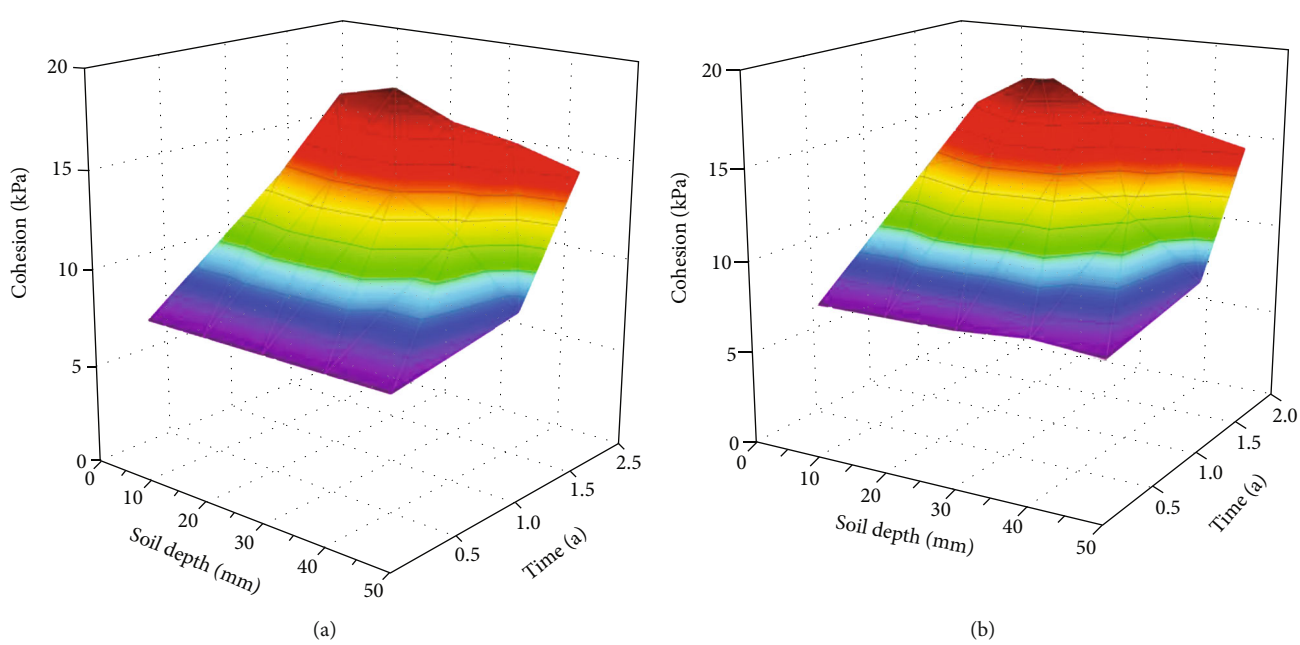

Figure 11: Cohesion of root-bearing soil at different growth periods and different depths: (a) test value; (b) predicted value.

wherem_1 is the number of severed roots in the roots.

$$\tau_f = 0.4 \cdot \sum_{i=0}^{m_1} \mathrm{RAR}_i \cdot T_i \cdot \left(\cos \alpha_i + \sin \alpha_i \tan \phi'\right) + (\sigma - u_a) \tan \phi' + (u_a - u_w)\left[\tan \phi' \left(\frac{\theta - \theta_r}{\theta_s - \theta_r}\right)\right]. \tag{11}$$

4.2.2. The Example Analysis. According to root damage in the direct shear test, root parameters (such as root geometry, tensile strength, Young's modulus, and root orientation) are shown in Table 7. The results of cohesion predicted by the model and the experimental results are shown in Figure 11. According to Wu, the root direction parameter is 1.2. As shown in Figure 11, the model prediction is in good agreement with the experimental results. Figure 11(a) shows the experimental results of cohesion of soil with roots at different depths, and Figure 11(b) shows the model prediction results. An acceptable agreement between the experimental and predicted values can be observed. These results verify that the mechanical effect of root system on soil reinforcement is a function of growth period and soil depth, and the proposed digital model can predict the experimental trend.

5. Conclusions

(1) D-W cycles had a significant effect on cohesion and internal friction angle ($P < 0.05$). With the number of D-W cycles increasing, the cohesive decreases; the internal friction angle is just the opposite

(2) The water content had a small effect on the internal friction angle but had a large effect on the cohesion. When the water content was less than 10%, the cohesion could be improved

(3) The factor levels of the large cohesive stage were as follows: the water content was 10%, VR content was 2%, dry density was 1.50 g/cm^3, and the number of D-W cycles was less than one

(4) Coal-bearing soils have many clay minerals and react violently with water. With the increase of D-W cycles, the links between mineral particles have a stable layered structure with unsteadiness chain structure

(5) The digital model of soil reinforcement by VR was established to quantify the enhancement effect of VR on the cohesion and shear strength of coal-bearing soils

Data Availability

The results of experimental data used to support the findings of this study are included within the supplementary materials (available here).

Conflicts of Interest

I, the corresponding author, am responsible for coauthors declaring their interests, and I declare that there is no conflict of interest regarding the publication of this article.

Acknowledgments

This research was funded by the National Natural Science Foundation of China (NSFC) [Grant no. 51568022] and Hubei Provincial Education Department Key Project [Grant no. 203201920903].

Supplementary Materials

The data in the first part of this section depicts stress-strain curves of vegetated coal-bearing soil specimens, as shown in Figure 5. The data in the second part of this section shows the change in cohesion of vegetated coal-bearing soil specimens according to influencing factor, as shown in Figure 6 in the manuscript. The data in the third part of this section shows the relationship between the number of D-W cycles and internal friction angle, as shown in Figure 7 in the manuscript. *(Supplementary Materials)*

References

[1] Z. Lei, "Stability analysis of coal measure soil slope under rainfall infiltration," *Rock and Soil Mechanics*, vol. 4, 2009.

[2] L. Zhu, S. Y. Han, B. N. Hong, and X. J. Song, "Analysis on stability of coal measure soil slope considering fissures and weathering under rainfall infiltration," *Journal of Water Resources and Architectural Engineering*, vol. 8, no. 4, pp. 86–89, 2010.

[3] L. Zhu and B.-N. Hong, "Sensitivity analysis on influencing factors of shallow landslide of coal measure strata," *Journal of Yangtze River Scientific Research Institute*, vol. 7, p. 17, 2011.

[4] L. Ji-dong, "Stability analysis and control of cutting high slopes in coal measure strata along Xiaotang-Gantang of Beijing-Zhuhai expressway," *Hydrogeology and Engineering Geology*, vol. 5, pp. 86–88, 2003.

[5] L. Zhu, X. J. Song, and B. N. Hong, "Analysis of shallow landslides stability of coal measure soil through contact elastic-plastic FEM," in *Advanced Materials Research*, pp. 2076–2083, Trans Tech Publications Ltd., 2011.

[6] L. Hui and L. Shunqing, "Comparative study on the water sensitivity of remoulded red clay and powered soil of coal measure strata," *Acta Scientiarum Naturalium Universitatis Sunyatseni*, vol. 54, no. 6, p. 89, 2015.

[7] X. Hu, B. N. Hong, Q. Du, and Y. M. Meng, "Influence of water contents on shear strength of coal-bearing soil," *Rock and Soil Mechanics*, vol. 30, no. 8, pp. 2291–2294, 2009.

[8] B. Han, G. Y. Lu, Z. Q. Zhu, Y. J. Guo, and Y. W. Zhao, "Microstructure features of powdery coal-bearing soil based on the digital image measurement technology and fractal theory," *Geotechnical and Geological Engineering*, vol. 37, no. 3, pp. 1357–1371, 2019.

[9] H. Zhang, W. Liao, J. Lin, B. Zhang, and H. Feng, "Correlation analysis of macroscopic and microscopic parameters of coal measure soil based on discrete element method," *Advances in*

Civil Engineering, vol. 2019, Article ID 1302682, 14 pages, 2019.

[10] H. Lei, Z. Peng, H. Yigang, and Z. Yang, "Vegetation and soil restoration in refuse dumps from open pit coal mines," *Ecological Engineering*, vol. 94, pp. 638–646, 2016.

[11] A. Kompała-Bąba, W. Bierza, A. Błońska et al., "Vegetation diversity on coal mine spoil heaps–how important is the texture of the soil substrate?," *Biologia*, vol. 74, no. 4, pp. 419–436, 2019.

[12] S. Sun, H. Sun, D. Zhang et al., "Response of soil microbes to vegetation restoration in coal mining subsidence areas at Huaibei coal mine, China," *International Journal of Environmental Research and Public Health*, vol. 16, no. 10, p. 1757, 2019.

[13] L. Harantová, O. Mudrák, P. Kohout, D. Elhottová, J. Frouz, and P. Baldrian, "Development of microbial community during primary succession in areas degraded by mining activities," *Land Degradation & Development*, vol. 28, no. 8, pp. 2574–2584, 2017.

[14] W. Li, J. Li, S. Liu et al., "Magnitude of species diversity effect on aboveground plant biomass increases through successional time of abandoned farmlands on the eastern Tibetan Plateau of China," *Land Degradation & Development*, vol. 28, no. 1, pp. 370–378, 2017.

[15] A. Gonzalez-Ollauri and S. B. Mickovski, "Hydrological effect of vegetation against rainfall-induced landslides," *Journal of Hydrology*, vol. 549, pp. 374–387, 2017.

[16] H. Liu, S. Feng, and C. Ng, "Analytical analysis of hydraulic effect of vegetation on shallow slope stability with different root architectures," *Computers and Geotechnics*, vol. 80, pp. 115–120, 2016.

[17] M. Bordoni, C. Meisina, A. Vercesi et al., "Quantifying the contribution of grapevine roots to soil mechanical reinforcement in an area susceptible to shallow landslides," *Soil and Tillage Research*, vol. 163, pp. 195–206, 2016.

[18] M. Y. Fattah, M. M. Al-Ani, and M. T. A. Al-Lamy, "Wetting and drying collapse behaviour of collapsible gypseous soils treated by grouting," *Arabian Journal of Geosciences*, vol. 8, no. 4, pp. 2035–2049, 2015.

[19] A. F. Jasim, M. Y. Fattah, I. F. al-Saadi, and A. S. Abbas, "Geogrid reinforcement optimal location under different tire contact stress assumptions," *International Journal of Pavement Research and Technology*, vol. 14, no. 3, pp. 357–365, 2021.

[20] E. T. Al-Taie, H. H. Al-Kalali, and M. Y. Fattah, "Evaluation of settlement and bearing capacity of embankment on soft soil with reinforced geogrids," *International Journal of Engineering Research & Technology*, vol. 8, no. 6, pp. 99–103, 2019.

[21] B. J. Nareeman and M. Y. Fattah, "Effect of soil reinforcement on shear strength and settlement of cohesive-frictional soil," *International Journal of Geomate*, vol. 3, no. 1, pp. 308–313, 2012.

[22] L. A. McGuire, F. K. Rengers, J. W. Kean et al., "Elucidating the role of vegetation in the initiation of rainfall-induced shallow landslides: insights from an extreme rainfall event in the Colorado Front Range," *Geophysical Research Letters*, vol. 43, no. 17, pp. 9084–9092, 2016.

[23] J. J. Ni, A. K. Leung, C. W. W. Ng, and W. Shao, "Modelling hydro-mechanical reinforcements of plants to slope stability," *Computers and Geotechnics*, vol. 95, pp. 99–109, 2018.

[24] T. S. Nguyen, S. Likitlersuang, and A. Jotisankasa, "Influence of the spatial variability of the root cohesion on a slope-scale stability model: a case study of residual soil slope in Thailand," *Bulletin of Engineering Geology and the Environment*, vol. 78, no. 5, pp. 3337–3351, 2019.

[25] H. Nowamooz and F. Masrouri, "Influence des cycles de succion sur la structure interne des sols gonflants argileux," *Comptes Rendus Geoscience*, vol. 342, no. 12, pp. 901–910, 2010.

[26] T. G. Sitharam, "Micromechanical modeling of granular materials: effect of confining pressure on mechanical behavior," *Mechanics of Materials*, vol. 31, no. 10, pp. 653–665, 1999.

[27] ASTM Committee D, *Standard Practice for Classification of Soils for Engineering Purposes (Unified Soil Classification System)*, ASTM International, West Conshohocken, PA, USA, 2011.

[28] C. W. W. Ng, A. Leung, and J. Ni, *Plant-Soil Slope Interaction*, CRC Press, 2019.

[29] C. W.-W. Ng, "Atmosphere-plant-soil interactions: theories and mechanisms," *Chinese Journal of Geotechnical Engineering*, vol. 39, pp. 1–47, 2017.

[30] F. Yilmaz and D. Fidan, "Effect of wetting-drying cycles on volumetric stability of clayey soil stabilized with lime and perlite," *European Journal of Technic*, vol. 7, no. 2, pp. 207–218, 2017.

[31] C. J. Wu and M. S. Hamada, *Experiments: Planning, Analysis, and Optimization*, John Wiley & Sons, 2011.

[32] T. Mori, *Taguchi Methods: Benefits, Impacts, Mathematics, Statistics, and Applications*, ASME Press, 2011.

[33] V. Vishal, P. Ranjith, and T. N. Singh, "An experimental investigation on behaviour of coal under fluid saturation, using acoustic emission," *Journal of Natural Gas Science and Engineering*, vol. 22, pp. 428–436, 2015.

[34] X. Yang, J. Wang, C. Zhu, M. He, and Y. Gao, "Effect of wetting and drying cycles on microstructure of rock based on SEM," *Environmental Earth Sciences*, vol. 78, no. 6, p. 183, 2019.

[35] A. Aldaood, M. Bouasker, and M. Al-Mukhtar, "Impact of wetting-drying cycles on the microstructure and mechanical properties of lime-stabilized gypseous soils," *Engineering Geology*, vol. 174, pp. 11–21, 2014.

[36] Z. Wu, Y. Deng, S. Liu, Q. Liu, Y. Chen, and F. Zha, "Strength and micro-structure evolution of compacted soils modified by admixtures of cement and metakaolin," *Applied Clay Science*, vol. 127-128, pp. 44–51, 2016.

[37] J. Berthonneau, P. Bromblet, F. Cherblanc, E. Ferrage, J. M. Vallet, and O. Grauby, "The spalling decay of building bioclastic limestones of Provence (South East of France): from clay minerals swelling to hydric dilation," *Journal of Cultural Heritage*, vol. 17, pp. 53–60, 2016.

[38] J. Berthonneau, O. Grauby, E. Ferrage et al., "Impact of swelling clays on the spalling decay of building limestones: insights from X-ray diffraction profile modeling," *European Journal of Mineralogy*, vol. 26, no. 5, pp. 643–656, 2014.

[39] J. Ruedrich, T. Bartelsen, R. Dohrmann, and S. Siegesmund, "Moisture expansion as a deterioration factor for sandstone used in buildings," *Environmental Earth Sciences*, vol. 63, no. 7-8, pp. 1545–1564, 2011.

[40] M. S. A. Perera, A. S. Ranathunga, and P. G. Ranjith, "Effect of coal rank on various fluid saturations creating mechanical property alterations using Australian coals," *Energies*, vol. 9, no. 6, p. 440, 2016.

[41] W. Polzer and J. Hem, "The dissolution of kaolinite," *Journal of Geophysical Research*, vol. 70, no. 24, pp. 6233–6240, 1965.

[42] F. Preti and M. Schwarz, "On root reinforcement modelling," *Geophysical Research Abstracts*, vol. 8, 2006.